Electrochemical Detection of Single-Nucleotide Mismatches: Application of M-DNA

E. Abu-Irhayem[*] Y-T. Long[*], T. Sutherland[*], C-Z Li[*], H-B Kraatz[*] and J. S. Lee[**]
[*] Department of Chemistry, University of Saskatchewan, 110 Science Place, Saskatoon, S7N 5C9
[**]Department of Biochemistry, University of Saskatchewan, 107 Wiggins Road, Saskatoon, S7N 5E5

ABSTRACT

The detection of a single-nucleotide mismatch in a 20 base pair duplex DNA, using EIS, is presented. Mismatched DNA monolayers on Au electrodes were studied as normal duplex DNA (B-DNA) and after conversion to Zn metalated duplex DNA (M-DNA). Modeling of the impedance data to an equivalent circuit provides parameters that are useful in discriminating each monolayer configuration. The conversion to M-DNA caused a decrease in the resistance to charge transfer (R_{CT}). Contrary to expectations, R_{CT} for B-DNA was also found to decrease for duplexes containing a mismatch. Dehybridization rehybridization studies to form DNA duplex with incomplete hybridization efficiencies showed that mismatch can still be detected for M-DNA but not for B-DNA. The R_{CT} for a perfect duplex was 76(12) Ohm•cm^2, whereas a mismatch in the middle of the sequence yielded a R_{CT} value of 30(15) Ohm•cm^2. The detection limit was measured and the impedance methodology reliably detected single DNA base pair mismatches at concentrations as low as 100 pM.

Keywords: DNA mismatch, biosensor, electrochemistry, impedance spectroscopy

1 INTRODUCTION

DNA biosensors have been the interest of many researchers in the past decade [1] due to its potential ability for rapid identification of base mutations or single nucleotide polymorphisms (SNP). [2] The simplest form of DNA chip consists of single-stranded DNA probes, attached to a surface in an array format. The target DNA is labeled with fluorescent tag and successful hybridization to an individual probe is detected fluorometrically. On the other hand, alternative methods of detection such as electrochemical ones can allow the direct readout of the electrical signal reducing the complexity of the sensor system. Barton and colleagues have developed a chronoamperometric technique that is utilizes the properties of the intercalator Methylene Blue (MB^+) which acts as a redox mediator between the DNA duplex attached to a gold electrode and the redox probe $[Fe(CN)_6]^{3-/4-}$ in solution. Duplex DNA containing a single-mismatch has a lower rate of charge transport and thus, can show a different response, compared to a perfect duplex.[3, 4] Heller and coworkers have used cyclic voltammetry (CV) to detect DNA mismatches at Au electrodes using a redox-active polymer adjacent to the Au surface and the covalent attachment of an enzyme to the target DNA sequence.[5, 6] Willner and coworkers used Electrochemical Impedance Spectroscopy (EIS) to detect mismatches in B-DNA (normal double-stranded-(ds)-DNA) by enzymatic amplification. [7, 8] Again, this uniquely sensitive technique relies on the covalent modification of the DNA. However, the weakness of such techniques is that they are affected by DNA hybridization efficiencies, and this can lead to erroneous conclusions.

Previously, we studied the conductivity of B-DNA and metalated DNA (M-DNA) at pH 8.6 using EIS and CV, showing that B-DNA can be converted to M-DNA by adding Zn^{2+} at pHs higher than 8.5. [9] In M-DNA, it is proposed that the metal ions replace the amino protons of guanine and thymine in every base pair, but the structure can be converted back to B-DNA by chelating the metal ions with EDTA, or by reducing the pH. Electron transport through M-DNA can be monitored by fluorescence spectroscopy of duplexes labeled at opposite ends with donor and acceptor chromophores. In EIS, the impedance of an electrode undergoing heterogeneous electron transfer through a self-assembled monolayer can be described using an equivalent electrical circuit consisting of resistance and capacitance elements, such as R_S (the solution resistance), R_{CT} (the charge transfer resistance), *CPE* (the constant-phase element) and a mass transfer element *W* (Warburg impedance). M-DNA formation causes significant changes in the electronic properties of the DNA that are readily detected by EIS. Nyquist plots show large differences between B- and M-DNA, which when analyzed by a modified Randle's circuit, demonstrate that the charge transfer resistance through the DNA is decreased for M-DNA. The charge transfer resistance increases with increasing duplex length for M-DNA, but in each case, the resistance for M-DNA is lower than its corresponding B-DNA construct. In addition, electron transfer is faster in M-DNA as compared to B-DNA. [9, 10] Applying the same principle, any kinks, bulges, caused by DNA mismatches can have a significant influence on the electronic coupling between the base pairs, leading to changes in the equivalent electrical circuit that represents the mismatched DNA system.

In this paper we present evidence that the presence and position of a single nucleotide mismatch in unlabeled M- and B-DNA monolayers causes characteristic changes in the impedance spectrum, which can be utilized for the detection of DNA mismatches, even low hybridization efficiencies, with a detection limit of 100 pM. This represents a significant improvement over other reported methods and demonstrates the utility of M-DNA.

2 EXPERIMENTAL

Materials: The 5'-disulfide-labeled and unlabeled oligonucleotide strands were synthesized by standard phosphoamidate solid-phase DNA synthesis using a fully automated DNA synthesizer, purified by reversed-phase HPLC and then characterized by electrospray ionization mass spectrometry (see supporting information).[9]

Monolayer Preparation: The freshly cleaned gold electrodes (BAS, 1.6 mm diameter) were incubated in 0.05 mM ss-DNA or ds-DNA B-DNA, 20 mM Tris-ClO_4 buffer solution (pH 8.6) for 5 days. Then the electrodes were washed with Tris-ClO_4 buffer and mounted into an electrochemical cell. Dehybridization and regeneration of the single-stranded probe electrode was achieved by denaturing the duplex DNA by soaking the electrode in a heated (60 ºC) water:EtOH (60:40) bath for 10 minutes then rinsing in room temperature 20 mM Tris-ClO_4 buffer. Reproducible behavior was found for repeated measurements on different electrodes. Rehybridization was performed by exposing the ss-DNA self-assembled monolayer (SAM) to SSC buffer (300 mM NaCl, 30 mM sodium citrate, pH 7) heated to 37 °C in the presence of target DNA for 10 minutes and then was allowed to cool to room temperature for an additional 3 hrs. B-DNA was converted to M-DNA by the addition of 0.4 mM $Zn(ClO_4)_2 \cdot 6\ H_2O$ for 2 hrs at pH 8.6.[9, 10]

The formation of the monolayer was assessed by standard blocking studies with $[Fe(CN)_6]^{3-/4-}$, X-Ray photoelectron spectroscopy (XPS) and EIS, as described previously.[9] The blocking studies showed a decrease in peak current attributed to the reduced diffusion of the redox probe to the Au surface. The XPS data shows the presence of a an Au-thiolate bond and a thickness of 44 Å for a **1**:**2** monolayer.[9]

Electrochemical measurements: A conventional three-electrode cell was used. All experiments were conducted at room temperature (22 °C). The cell was enclosed in a grounded Faraday cage. The reference electrode was constructed by sealing a Ag/AgCl wire into a glass tube with a solution of 3 M KCl that was capped with a Vycor tip. The counter electrode was a platinum wire. Impedance spectra were measured using an EG&G 1025 frequency response analyzer interfaced to an EG&G 283 potentiostat/galvanostat. The AC voltage amplitude was 5 mV and the voltage frequencies used for EIS measurements ranged from 100 kHz to 100 mHz. The applied potential was 250 mV vs. Ag/AgCl, (formal potential, E^0, of the redox probe $[Fe(CN)_6]^{3-/4-}$. All measurements were repeated a minimum of 5 times with separate electrodes to obtain statistically meaningful results.

3 RESULTS AND DISCUSSION

Monolayers of fully matched B-DNA on gold were prepared from the oligonucleotide **1** and its fully matched complementary strand **2**. The properties of the resulting **1**:**2** B-DNA surface compares well with those described before.[9, 10] 3 types of mismatched monolayers were prepared in order to evaluate the effect of mismatches by EIS, Each monolayer contained a single pyrimidine-pyrimidine mismatch in the complementary strand. Complementary mismatched strand **3** contains a mismatch in the second top base pair, resulting in a mismatch distal to the electrode surface. Complementary mismatched strand **4** contains a T instead of a G in position 11, giving a monolayer with the mismatch in the middle of the duplex. Complementary mismatched strand **5** possesses a C instead of an A in position 19, resulting in a mismatch proximal to the electrode surface. Mismatched B-DNA monolayers of **1**:**3**, **1**:**4**, and **1**:**5** were prepared in an analogous manner (see Figure 1).

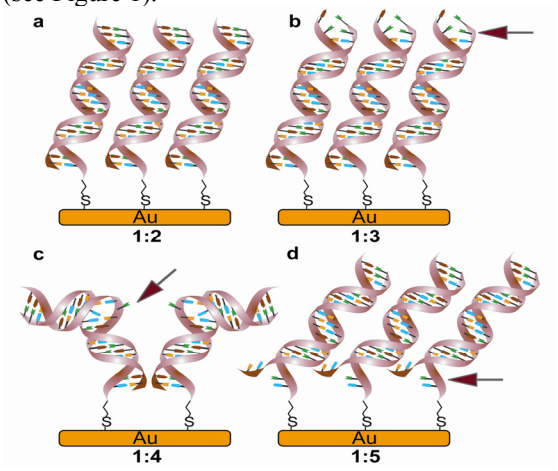

Figure 1. Proposed structures of the monolayers prepared in this study. a) **1**:**2**, the complementary ds-DNA monolayer. b) **1**:**3**, mismatch distal to the Au surface of the ds-DNA monolayer. c) **1**:**4**, mismatch in the middle of the ds-DNA monolayer. d) **1**:**5**, mismatch proximal to the Au surface of the ds-DNA monolayer. The arrow indicates the position of the mismatched base pair.

EIS measurements were carried out on all monolayers in 20 mM Tris-ClO_4 (pH 8.6) in the presence of 4 mM $[Fe(CN)_6]^{3-/4-}$ (1:1) mixture, as the solution-based redox probe. The B-DNA monolayers were then converted to M-DNA monolayers by the addition of 0.4 mM Zn^{2+} at pH 8.6 as described before.[9, 10] The impedance measurements were repeated under M-DNA conditions for all four monolayers. Control experiments were performed with longer incubation times with Zn^{2+} and repeated EIS measurements. Neither procedure produced changes in the impedance spectra demonstrating that the DNA was not significantly damaged, for example, by oxidation due to electron transfer [15]. Typical impedance spectra, in the form of Nyquist plots, for B-DNA and M-DNA monolayers of a perfectly matched duplex (**1**:**2**) and a duplex containing a mismatch in the middle of the helix (**1**:**4**) are shown in Figure 2. Each point represents a value of Z_{im} and Z_{re} measured at a particular AC frequency. The spectra show lower impedance for M-DNA than for B-

DNA, as would be expected from previous observations. [9-13] More importantly, the presence of a mismatch in the DNA duplex decreases the impedance of B-DNA while increasing the impedance of M-DNA. In order to provide a rationale for this behavior, the impedance spectra of all DNA films were analyzed with a modified Randles equivalent circuit. [9] The circuit drawing is shown in Figure 2. The same model was used to fit all monolayers described here. The fit of the equivalence circuit to the experimental values is given as a solid line. This treatment allows the interpretation of the impedance data in terms of electronic circuit components The equivalent circuit contains five elements that are described below.

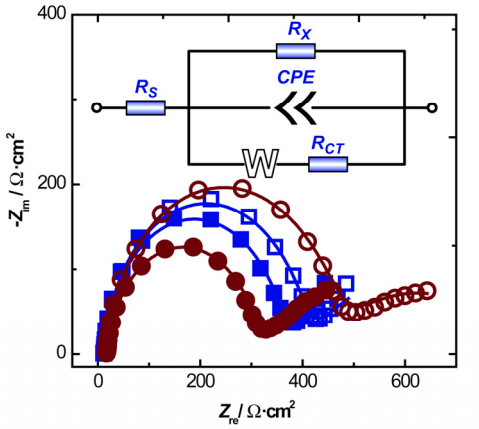

Figure 2. Nyquist plots ($-Z_{im}$ vs. Z_{re}) of the 20 base pair complementary B-DNA (○), middle mismatch B-DNA(□), complementary M-DNA(●)and middle mismatch M-DNA(■) assembled on gold in 4 mM $[Fe(CN)_6]^{3-/4-}$ (1:1) mixture as the redox probe in 20 mM Tris-ClO_4 and 20 mM $NaClO_4$ solution. Applied potential of 250 mV versus Ag/AgCl. $[Zn^{II}]$ = 0.4 mM; pH 8.6. In all cases the measured data points are shown as symbols with the calculated fit to the equivalent circuit as solid lines. Inset: The experimental data were fit to the equivalent circuit. R_S: solution resistance, R_X: monolayer pinhole/defect resistance, R_{CT}: charge transfer resistance, *CPE*: constant phase element, *W*: Warburg impedance.

A solution resistance term, R_S, remains constant at 5-6 Ω·cm^2 as would be expected for measurements under identical conditions of supporting electrolyte concentration and temperature. The circuit contains a constant phase element (*CPE*) acting as a non-ideal capacitor, which is commonly used instead of a capacitor to account for the interface between solution and electrode surface.[14] Here, the *CPE* will be interpreted as a capacitor as described elsewhere in situations where the exponential modifier is greater than 0.9,[15] which is the case for all monolayers presented in this paper. CPE is influenced by the monolayer composition and thickness. The magnitude of the *CPE* for films of the matched duplex **1**:**2** and the two top and bottom mismatched duplexes **1**:**3** and **1**:**5** are in the range of 10 – 25 μF.cm^{-2}. However, for films of **1**:**4**, B- and M-DNA containing the middle mismatch, a significantly higher capacitance of about 40 (2) μF.cm^{-2} was observed. This can be attributed to possible change in the monolayer thickness for films of **1**:**4** due to kinking of the helix, which is caused by the mismatch in the centre of the DNA sequence. This kink will cause the duplex to bend towards the surface resulting in a decrease in the film thickness. The top and bottom mismatch containing films, **1**:**3** and **1**:**5**, respectively, yield CPE values that also indicate slight variations in the thickness of the monolayer due to fraying of the strands for both films. However, the effects of fraying for the top and bottom mismatch films are opposite. Fraying in the top of the helix will result in a better interaction between individual non-paired base pairs and the solvent, thus leading to a thicker monolayer. In the case of the mismatch being proximal to the electrode surface, as for film **1**:**5**, fraying is expected to enhance flexibility of the DNA-linker region, which may result in a lower film thickness by compaction.

The R_X component of the equivalence circuit can be attributed to pinholes in the monolayer structure. The value of R_X is similar for each of the B-DNA monolayers, indicating the number and size of the pinholes does not change between monolayers. However, R_X tends to decrease upon conversion to M-DNA. This behavior can be attributed to M-DNA having a slightly more compact structure than B-DNA due to the divalent metal ions reducing the repulsion between the phosphate backbone residues of adjacent helices.[9, 10, 12, 13] The Warburg impedance element, *W*, is dependent on the rate of diffusion of the $[Fe(CN)_6]^{3-/4-}$ redox probe. The Warburg impedance is smallest for the perfect duplex in the B-DNA conformation suggesting that this is the most ordered monolayer, which offers the least access of the solution electrophore through the DNA monolayer.

The charge transfer resistance term, R_{CT}, comprises resistance terms resulting from (a) transfer of the electron from the $[Fe(CN)_6]^{3-/4-}$ redox probe to the DNA monolayer, (b) the resistance to charge transfer between the base pairs of the DNA helix and (c) from the helix to the surface of the gold electrode. As expected, for all monolayers, R_{CT} is lower for M-DNA than B-DNA. More importantly, R_{CT} allows the discrimination between a single nucleotide mismatch and a perfectly-matched DNA film. The presence of a mismatch causes a decrease in R_{CT} for all films containing mismatches. This is contrary to expectations since the electron transfer (ET) kinetics through an unstacked region is retarded.[3, 4, 16] Therefore, thickness and/or disorder in the monolayer, as signified by the changes in the *CPE* term, must dominate rates of ET rather than simple R_{CT}. As far as mismatch detection is concerned, the evaluation of the difference in charge transfer resistance, ΔR_{CT}, between B- and M-DNA for a given film gives excellent discrimination between a perfect duplex and one containing a single mismatch at either the top or middle positions of the duplex. ΔR_{CT} for the perfectly matched duplex film **1**:**2** is 190 (22) Ω.cm^2

whereas for the mismatched films, ΔR_{CT} is significantly smaller. Interestingly, ΔR_{CT} for the top mismatch containing film of **1**:**3** and the bottom mismatch (**1**:**5**) are similar (95(19) $\Omega.cm^2$ for **1**:**3** and 85(20) $\Omega.cm^2$ for **1**:**5**). ΔR_{CT} for the duplex containing the middle mismatch is much lower (30(18) $\Omega.cm^2$ for **1**:**4**). The use of ΔR_{CT} was attractive from an application perspective because different electrode morphologies can yield different impedances but the comparative impedance measurements between B- and M-DNA are reproducible.

To examine the ability for mismatch determination under non-ideal conditions, dehybridization and rehybridization studies were carried out (see experimental section) to form target DNA with rehybridization efficiencies between 40-70 %. It was found that, despite the incomplete rehybridization, and even at low rehybridization efficiencies, the mismatch can still be detected in the M-DNA target. However, for B-DNA films, the matched and mismatched rehybridized DNA targets were indistinguishable. This may be attributed to the role of Zn^{2+} in M-DNA, which is able to bind and alter the electronic properties of duplex DNA without altering electronically the ss-DNA monolayers. Therefore, incomplete hybridization did not have a significant effect on mismatch detection in M-DNA monolayers.

Finally, rehybridization experiments were carried out at various concentrations of target complementary strand to determine the minimum concentration of target ss-DNA required to discriminate a matched film from a mismatched DNA film. Each time, the impedance spectra were recorded for B- and M-DNA films and fit to the equivalent circuit described in Fig. 2. ΔR_{CT} remains relatively constant down to concentrations of 100 pM of target ss-DNA. It is important to emphasize that a clear discrimination between matched and mismatched DNA is obtained by the difference in R_{CT} between B- and M-DNA.

4 CONCLUSIONS

Although this study has been limited to the detection of a pyrimidine pyrimidine mismatch, purine purine mismatches should also be detectable since they cause even larger disruptions to the helical stack of a DNA duplex. The presence of a mismatch causes a decrease in R_{CT} regardless of the position of the mismatch. The difference in charge transfer resistance, ΔR_{CT}, between B- and M-DNA represents a reliable measure of the presence of a single nucleotide mismatch under ideal conditions. Even under conditions in which incomplete hybridization is observed, single nucleotide mismatches can be detected by the formation of M-DNA. Thus, these results present a significant step forward in the electrochemical detection of SNPs using an unlabeled DNA hybrid.

A device with a detection limit of 100 pM can potentially be used for such applications as clinical diagnosis of mutations. However, an amplification step to increase DNA concentrations from biological samples is required before this sensor can be utilized. In the long term, better sensitivity can be obtained by utilizing working electrodes that are much smaller in size.. For example, if a 1.5 mm diameter electrode can detect 100 pM of target then a 1.5 μ electrode would have a sensitivity in the femtomolar range at which point direct detection without amplification of the target becomes realistic.

This work was not possible without the CHIR, NSERC, and UMDI financial support. H-B Kraatz is the Canada Research Chair in Biomaterials and J.S Lee is supported by a Senior Investigators Award from the Regional Partnership Program of CHIR. Special thanks also to Don Schwab at the Plant Biotechnology Institute, Saskatchewan, Canada for the preparation of DNA samples.

REFERENCES

[1] I. Willner, *Science* **2002**, *298*, 2407.
[2] A. Brookes, *Gene* **1999**, *234*, 177.
[3] E. M. Boon, D. M. Ceres, T. G. Drummond, M. G. Hill, J. K. Barton, *Nat. Biotech.* **2000**, *18*, 1096.
[4] S. O. Kelley, E. M. Boon, J. K. Barton, N. M. Jackson, M. G. Hill, *Nucleic Acids Res.* **1999**, *27*, 4830.
[5] G. Hartwich, D. J. Caruana, T. de Lumley-Woodyear, Y. Wu, C. N. Campbell, A. Heller, *J. Am. Chem. Soc.* **1999**, *121*, 10803.
[6] D. J. Caruana, A. Heller, *J. Am. Chem. Soc.* **1999**, *121*, 769.
[7] F. Patolsky, A. Lichtenstein, I. Willner, *Nature Biotech.* **2001**, *19*, 253.
[8] F. Patolsky, Y. Weizmann, E. Katz, I. Willner, *Angew. Chem., Int. Ed.* **2003**, *42*, 2372.
[9] Y.-T. Long, C.-Z. Li, H.-B. Kraatz, J. S. Lee, *Biophys. J.* **2003**, *84*, 3218.
[10] C.-Z. Li, Y.-T. Long, H.-B. Kraatz, J. S. Lee, *J. Phys. Chem. B* **2003**, *107*, 2291.
[11] A. Rakitin, P. Aich, C. Papadopoulos, Y. Kobzar, A. S. Vedeneev, J. S. Lee, J. M. Xu, *Phys. Rev. Lett.* **2001**, *86*, 3670.
[12] P. Aich, S. L. Labiuk, L. W. Tari, L. J. T. Delbaere, W. J. Roesler, K. J. Falk, R. P. Steer, J. S. Lee, *J. Mo.l Biol.* **1999**, *294*, 477.
[13] J. S. Lee, L. J. P. Latimer, R. S. Reid, *Biochem. Cell Biol.* **1993**, *71*, 162.
[14] M. Dijksma, B. A. Boukamp, B. Kamp, W. P. van Bennekom, *Langmuir* **2002**, *18*, 3105.
[15] S. E. Creager, T. T. Wooster, *Ana.l Chem.* **1998**, *70*, 4257.
[16] S. O. Kelley, N. M. Jackson, M. G. Hill, J. K. Barton, *Angew Chem., Int. Ed.* **1999**, *38*, 941.